

# 3-D THEORY OF A HIGH GAIN FREE-ELECTRON LASER BASED ON A TRANSVERSE GRADIENT UNDULATOR

Panagiotis Baxevanis, Yuantao Ding, Zhirong Huang and Ronald Ruth  
SLAC National Accelerator Laboratory, Menlo Park, CA 94025, USA

## Abstract

The performance of a free-electron laser (FEL) depends significantly on the various parameters of the driving electron beam. In particular, a large energy spread in the beam results in a substantial reduction of the FEL gain, an effect which is especially relevant when one considers FELs driven by plasma accelerators or storage rings. For such cases, one possible solution is to use a transverse gradient undulator (TGU). In this concept, the energy spread problem is mitigated by properly dispersing the electron beam and introducing a linear, transverse field dependence in the undulator. This paper presents a self-consistent theoretical analysis of a TGU-based high gain FEL, taking into account three-dimensional (3-D) effects and beam size variations along the undulator. The results of our theory compare favorably with simulation and are used in fast optimization studies of various X-ray FEL configurations.

## INTRODUCTION

In recent years, the free-electron laser (FEL) has demonstrated its value as a tunable source of intense, coherent X-rays. In order to achieve the desired quality for the output radiation, a high-brightness electron beam is required to drive the machine. Electron beams from laser-plasma accelerators (LPAs) and ultimate storage rings (USRs) are characterized by low emittance and (in the case of the former) very high peak current, which would make them attractive for FEL applications. Unfortunately, they also have a relatively large energy spread, which poses a problem as far as their use in FELs is concerned. That is because a large spread in the energy of the electrons translates into a significant spread in the resonant wavelength, exceeding the FEL bandwidth. In this paper, we focus on one proposed solution, namely the transverse gradient undulator (TGU). The latter is an undulator with canted magnetic poles, so that its vertical field has a linear dependence upon the horizontal position  $x$ . Using a suitable dispersive element, one can also introduce a linear correlation of the electron energy with  $x$ . By properly selecting the parameters involved, one can ensure that electrons with higher than nominal energy are dispersed towards the higher-field region in such a way that the variation in the resonant frequency is minimized.

Originally conceived as a way to increase the energy acceptance of low gain (oscillator) FELs ([1]-[2]), the TGU has recently been considered in the context of its possible application in high gain devices. In particular, Ref. [3] developed a 1-D theoretical model and examined 3-D effects

through simulation. Here, we present a theoretical description of a TGU-based FEL in the framework of the Vlasov-Maxwell formalism, including 3-D effects due to the transverse electron beam size and emittance. Starting from the single particle equations of motion, a self-consistent equation for the amplitude of the radiation is derived using the Vlasov-Maxwell equations. Whenever applicable, we show how a simple solution can be obtained in terms of the eigenmodes of the system.

## THEORY

### Single Particle Motion

In our analysis, we assume that the magnetic field of the TGU is given by

$$\begin{aligned} B_{ux} &= B_0 \frac{\alpha}{k_u} \sinh(k_u y) \sin(k_u z) \\ B_{uy} &= B_0 (1 + \alpha x) \cosh(k_u y) \sin(k_u z) \\ B_{uz} &= B_0 (1 + \alpha x) \sinh(k_u y) \cos(k_u z), \end{aligned} \quad (1)$$

where  $k_u = 2\pi/\lambda_u$  ( $\lambda_u$  is the undulator period),  $B_0$  is the peak on-axis field and  $\alpha$  is the transverse field gradient, which can be related to the cant angle of the undulator poles. This magnetic field satisfies Maxwell's equations and reduces to the field of a standard, flat-pole undulator for  $\alpha \rightarrow 0$ . As we have already mentioned, the object of the TGU is to mitigate the negative impact of a large energy spread in the electron beam by significantly reducing the resulting spread in the resonant wavelength. In order to achieve this, the beam is dispersed in the  $x$ -direction so that the horizontal position of an electron is linearly correlated to its energy  $\gamma mc^2$  according to  $x = \eta \delta$ , where  $\delta = \gamma/\gamma_0 - 1$  is the energy deviation and  $\gamma_0 mc^2$  is the average electron energy. On the other hand, the introduction of the constant field gradient  $\alpha$  leads to a linear  $x$ -dependence of the undulator parameter  $K$ , i.e.  $K = K_0(1 + \alpha x)$ , where  $K_0 = eB_0/(mck_u)$  is its on-axis value ( $e$  is the electron charge). By selecting the dispersion function  $\eta$  as

$$\eta = \frac{2 + K_0^2}{\alpha K_0^2}, \quad (2)$$

the resonant condition  $\lambda_r = \lambda_u(1 + K^2/2)/(2\gamma^2)$  is now satisfied by all the electrons in the beam (up to linear order in  $x$ ).

For a detailed derivation of the single particle equations of motion, we refer to [4]. Here, we merely quote the main results. As far as the transverse dynamics is concerned, the TGU is characterized by a horizontal focusing strength

$k_\beta \sim (\eta\gamma_0)^{-1}$ . In this paper, we assume that this focusing effect is weak ( $k_\beta L_u \ll 1$ , where  $L_u$  is the undulator length) and exclude it from our analysis. However, we do take into account the vertical natural focusing of the undulator, whose strength  $k_n$  is given by  $k_n \approx K_0 k_u / (\sqrt{2}\gamma_0)$ . Thus, the transverse equations of motion for an electron are  $x'' = 0$  and  $y'' = -k_n^2 y$ , or, in a more canonical form,

$$\begin{aligned} \frac{dx}{dz} &= p_x & \frac{dp_x}{dz} &= 0, \\ \frac{dy}{dz} &= p_y & \frac{dp_y}{dz} &= -k_n^2 y. \end{aligned} \quad (3)$$

Moreover, we express the electric field of the linearly polarized radiation as

$$E_x = \frac{1}{2} \int_0^\infty d\nu E_\nu(\mathbf{x}, z) e^{i\nu k_r(z-ct)} + c.c., \quad (4)$$

where  $\nu = \omega/\omega_r$ ,  $E_\nu$  is the radiation amplitude,  $\mathbf{x} = (x, y)$ ,  $\omega_r = ck_r = 2\pi c/\lambda_r = 2\gamma_0^2 ck_u/(1+a_w^2)$  is the resonant frequency ( $a_w = K_0/\sqrt{2}$ ) and  $c.c.$  stands for complex conjugate. The pendulum equations for the longitudinal motion are

$$\frac{d\theta}{dz} = \theta' = 2k_u(\delta - \frac{x}{\eta}) - \frac{k_r}{2}(p_x^2 + p_y^2 + k_n^2 y^2) \quad (5)$$

and

$$\frac{d\delta}{dz} = \kappa_1 \int_0^\infty d\nu E_\nu(\mathbf{x}, z) e^{-i\Delta\nu k_u z} e^{i\nu\theta} + c.c.. \quad (6)$$

Here,  $\theta = k_u z + k_r(z - ct)$  is the averaged electron phase,  $\Delta\nu = \nu - 1$  is the detuning parameter and  $\kappa_1 = eK_0[JJ]/(4\gamma_0^2 mc^2)$  - where  $[JJ] = J_0(Q_0) - J_1(Q_0)$ , with  $Q_0 = K_0^2/(4 + 2K_0^2)$ , is the well known factor arising from the wiggles averaging. We note the presence of the linear term proportional to  $x$  on the RHS of Eq. (5), which reflects the resonant character of particles with  $x = \eta\delta$ .

### Vlasov-Maxwell Equations

Following the standard perturbation approach [5], we find that the linearized, frequency-domain Vlasov equation for the FEL is

$$\begin{aligned} \frac{\partial f_\nu}{\partial z} + p_x \frac{\partial f_\nu}{\partial x} + p_y \frac{\partial f_\nu}{\partial y} - k_n^2 y \frac{\partial f_\nu}{\partial p_y} + i\nu\theta' f_\nu \\ = -\kappa_1 \frac{\partial f_0}{\partial \delta} E_\nu e^{-i\Delta\nu k_u z}, \end{aligned} \quad (7)$$

where  $f_\nu$  is the Fourier amplitude of the perturbation  $f_1$  to the beam distribution function. Furthermore, the unperturbed distribution  $f_0$  satisfies the relation

$$\frac{\partial f_0}{\partial z} + p_x \frac{\partial f_0}{\partial x} + p_y \frac{\partial f_0}{\partial y} - k_n^2 y \frac{\partial f_0}{\partial p_y} = 0. \quad (8)$$

On the other hand, the evolution of the radiation field is governed by the paraxial wave equation

$$\left( \frac{\partial}{\partial z} + \frac{\nabla_\perp^2}{2i\nu k_r} \right) E_\nu = -\kappa_2 e^{i\Delta\nu k_u z} \int dp_x dp_y \int d\delta f_\nu, \quad (9)$$

where  $\kappa_2 = eK_0[JJ]/(2\epsilon_0\gamma_0) - \epsilon_0$  is the vacuum permittivity. Eqs. (7)-(9) accurately describe the FEL interaction in the linear regime. Using the method of integration along the unperturbed trajectories ([5],[6]), Eq. (7) can be solved in terms of  $f_\nu$ , yielding

$$\begin{aligned} f_\nu = -\kappa_1 \frac{\partial f_0}{\partial \delta} \int_0^z d\zeta E_\nu(x_+, y_+, \zeta) e^{-i\Delta\nu k_u \zeta} \\ \times \exp [i\nu(\theta'\xi - (k_u p_x/\eta)\xi^2)] \end{aligned} \quad (10)$$

for an initially unmodulated electron beam. In the equation given above, we have defined  $\xi = \zeta - z$ ,  $x_+ = x + p_x \xi$  and  $y_+ = y \cos(k_n \xi) + (p_y/k_n) \sin(k_n \xi)$ . We then choose a background distribution that corresponds to a dispersed beam with a constant size in the  $y$ -direction and a uniform longitudinal profile, i.e.

$$\begin{aligned} f_0 = \frac{N_b/l_b}{(2\pi)^{5/2} \sigma_x \sigma_y \sigma'_x \sigma'_y \sigma_\delta} \\ \times \exp \left[ -\frac{(x - \eta\delta - p_x z_x)^2}{2\sigma_x^2} - \frac{p_x^2}{2\sigma'_x{}^2} \right] \\ \times \exp \left[ -\frac{y^2}{2\sigma_y^2} - \frac{p_y^2}{2\sigma'_y{}^2} \right] \exp \left[ -\frac{\delta^2}{2\sigma_\delta^2} \right]. \end{aligned} \quad (11)$$

In the above relation,  $l_b$  and  $N_b$  are the bunch length and the total number of electrons,  $\sigma_\delta$  is the rms energy spread,  $z_x = z - z_0$  ( $z_0$  is a constant offset) while  $\sigma_{x,y}$  and  $\sigma'_{x,y}$  are the rms values for the beam size and the divergence at  $z_x = 0$  (in the absence of dispersion). Note that  $\sigma'_y/\sigma_y = k_n$  and that the beam emittance values are  $\epsilon_{x,y} = \sigma_{x,y} \sigma'_{x,y}$ . Inserting Eq. (10) into the RHS of Eq. (9) and performing the  $\delta$ -integration, we obtain a self-consistent equation for the amplitude of the radiation:

$$\begin{aligned} \left( \frac{\partial}{\partial z} + \frac{\nabla_\perp^2}{2ik_r} \right) E_\nu = -\frac{8i\rho_T^3 k_u^3}{2\pi\sigma'_x \sigma'_y} \int_0^z d\zeta \xi e^{-i\Delta\nu k_u \zeta} \\ \times \exp \left[ -2(\sigma_\delta^{ef})^2 k_u^2 \xi^2 \right] \int dp_x dp_y E_\nu(x_+, y_+, \zeta) \\ \times \exp \left[ 2ik_u \xi \left( -\frac{\sigma_x^2 x}{\sigma_T^2 \eta} - \frac{p_x}{\eta} \left( \frac{\xi}{2} + \left( 1 - \frac{\sigma_x^2}{\sigma_T^2} \right) z_x \right) \right) \right] \\ \times \exp \left[ -\frac{(x - p_x z_x)^2}{2\sigma_T^2} - \frac{1}{2} \left( \frac{1}{\sigma'_x{}^2} + ik_r \xi \right) p_x^2 \right. \\ \left. - \frac{1}{2} \left( \frac{1}{\sigma'_y{}^2} + ik_r \xi \right) (p_y^2 + k_n^2 y^2) \right]. \end{aligned} \quad (12)$$

Here,

$$\sigma_T = (\sigma_x^2 + \eta^2 \sigma_\delta^2)^{1/2} = \sigma_x \left( 1 + \frac{\eta^2 \sigma_\delta^2}{\sigma_x^2} \right)^{1/2} \quad (13)$$

is the total horizontal beam size in the absence of emittance,

$$\rho_T = \rho \left( 1 + \frac{\eta^2 \sigma_\delta^2}{\sigma_x^2} \right)^{-1/6} \quad (14)$$

is the corresponding attenuated FEL parameter and  $\sigma_\delta^{ef}$  is a (reduced) effective energy spread given by

$$\frac{1}{(\sigma_\delta^{ef})^2} = \frac{1}{\sigma_\delta^2} + \frac{\eta^2}{\sigma_x^2} \rightarrow \sigma_\delta^{ef} = \sigma_\delta \left(1 + \frac{\eta^2 \sigma_\delta^2}{\sigma_x^2}\right)^{-1/2}. \quad (15)$$

Efficient operation of the TGU requires  $\eta\sigma_\delta/\sigma_x \gg 1$ , so we usually approximate  $\sigma_\delta^{ef} \approx \sigma_x/\eta$ . The FEL parameter  $\rho$  in absence of dispersion is given by

$$\rho = \left(\frac{I_p}{16I_A} \frac{K_0^2 [JJ]^2}{\gamma_0^3 \sigma_x \sigma_y k_u^2}\right)^{1/3}, \quad (16)$$

where  $I_p = ecN_b/l_b$  is the peak current and  $I_A \approx 17$  kA is the Alfven current. Eq. (12) incorporates all the three-dimensional effects under consideration, including the variation of the horizontal beam size with  $z$ .

### Eigenmode Formalism

The case of vanishing horizontal emittance (i.e. when  $\sigma'_x \rightarrow 0$  but  $\sigma'_y \neq 0$ ) is relevant for FELs based on electron beams from ultimate storage rings and also allows for a simpler description in terms of guided modes of the form  $E_\nu = A(\mathbf{x})e^{i\mu z}$ , where  $\mu$  is the (constant) complex growth rate and  $A(\mathbf{x})$  is the mode profile. In particular, we find that the eigenmode equation is

$$\begin{aligned} \left(\mu - \frac{\nabla_\perp^2}{2k_r}\right) A(\mathbf{x}) &= -\frac{8\rho_T^3 k_u^3}{\sqrt{2\pi}\sigma_y} \exp\left(-\frac{x^2}{2\sigma_T^2}\right) \\ &\times \int_{-\infty}^0 d\xi \xi \frac{e^{i(\mu - \Delta\nu k_u)\xi}}{|\sin(k_n \xi)|} \exp\left[-2(\sigma_\delta^{ef})^2 k_u^2 \xi^2\right] \\ &\times \exp\left(-2ik_u \xi \frac{\sigma_x^2 x}{\sigma_T^2 \eta}\right) \int dy_+ A(x, y_+) \\ &\times \exp\left[-\frac{(1 + ik_r \sigma_y'^2 \xi)(y_+^2 + y^2 - 2yy_+ \cos(k_n \xi))}{2\sigma_y^2 \sin^2(k_n \xi)}\right]. \end{aligned} \quad (17)$$

We employ a variational technique in order to obtain an approximate solution for the fundamental mode [7]. Assuming a trial solution of the form  $A(\mathbf{x}) = \exp(-a_x x^2 + bx) \exp(-a_y y^2)$  - where the linear  $bx$  term in the exponent has been added to account for the asymmetry in the integral kernel of Eq. (17) under the reflection  $x \rightarrow -x$  - we multiply both sides of the above equation by  $A(\mathbf{x})$  and integrate over the transverse position. The result is the relation

$$\begin{aligned} \mu + \frac{a_x + a_y}{2k_r} &= -8\rho_T^3 k_u^3 \frac{\sqrt{a_x} \sqrt{a_y}}{\sqrt{a_x + 1/(4\sigma_T^2)}} \\ &\times \int_{-\infty}^0 d\xi \xi \exp\left(\frac{(b - ik_u \xi (\sigma_x^2/\sigma_T^2) \frac{1}{\eta})^2}{2a_x + 1/(2\sigma_T^2)} - \frac{b^2}{2a_x}\right) \\ &\times e^{i(\mu - \Delta\nu k_u)\xi} \exp\left[-2(\sigma_\delta^{ef})^2 k_u^2 \xi^2\right] / [a_y^2 \sigma_y^2 \sin^2(k_n \xi) \\ &+ a_y(1 + ik_r \sigma_y'^2 \xi) + (1/(4\sigma_y^2))(1 + ik_r \sigma_y'^2 \xi)^2]^{1/2}. \end{aligned} \quad (18)$$

Using Eq. (18) in conjunction with  $\partial\mu/\partial a_x = 0$ ,  $\partial\mu/\partial b = 0$  and  $\partial\mu/\partial a_y = 0$ , we obtain an approximation to the fundamental growth rate and mode profile. If the emittance in both directions is sufficiently small, we can employ a parallel beam model for both  $x$  and  $y$ , in which case Eq. (18) reduces to

$$\begin{aligned} \mu + \frac{a_x + a_y}{2k_r} &= -8\rho_T^3 k_u^3 \frac{\sqrt{a_x} \sqrt{a_y}}{\sqrt{a_x + 1/(4\sigma_T^2)} \sqrt{a_y + 1/(4\sigma_y^2)}} \\ &\times \int_{-\infty}^0 d\xi \xi e^{i(\mu - \Delta\nu k_u)\xi} \exp\left[-2(\sigma_\delta^{ef})^2 k_u^2 \xi^2\right] \\ &\times \exp\left(\frac{(b - ik_u \xi (\sigma_x^2/\sigma_T^2) \frac{1}{\eta})^2}{2a_x + 1/(2\sigma_T^2)} - \frac{b^2}{2a_x}\right). \end{aligned} \quad (19)$$

The integral on the RHS of the above relation can be expressed in terms of error functions, allowing for faster numerical calculations. In particular, we find

$$\begin{aligned} \mu + \frac{a_x + a_y}{2k_r} &= -8\rho_T^3 k_u^3 \frac{\sqrt{a_x} \sqrt{a_y}}{\sqrt{a_x + 1/(4\sigma_T^2)} \sqrt{a_y + 1/(4\sigma_y^2)}} \\ &\times e^{A_0} \left[ \frac{\sqrt{\pi} A_1}{4A_2^{3/2}} \exp\left(\frac{A_1^2}{4A_2}\right) \text{Erfc}\left(\frac{A_1}{2A_2^{1/2}}\right) - \frac{1}{2A_2} \right], \end{aligned} \quad (20)$$

where  $\text{Erfc}(x) = 1 - (2/\sqrt{\pi}) \int_0^x e^{-t^2} dt$  is the complementary error function and

$$\begin{aligned} A_0 &= -\frac{b^2}{4a_x(2a_x\sigma_T^2 + 1/2)}, \\ A_1 &= i[\mu - \Delta\nu k_u - 2\frac{\sigma_x^2}{\sigma_T^2} \frac{k_u b/\eta}{2a_x + 1/(2\sigma_T^2)}], \\ A_2 &= \frac{\sigma_x^4}{\sigma_T^4} \frac{(k_u/\eta)^2}{2a_x + 1/(2\sigma_T^2)} + 2(\sigma_\delta^{ef})^2 k_u^2. \end{aligned} \quad (21)$$

Once the growth rate and the mode parameters are known, one can calculate the power gain length  $L_g = -1/(2\Im[\mu])$  as well as the mode sizes  $\sigma_{rx} = (4\text{Re}[a_x])^{-1/2}$  and  $\sigma_{ry} = (4\text{Re}[a_y])^{-1/2}$ .

## NUMERICAL RESULTS

To illustrate our theoretical analysis, we have used two FEL parameter sets, both of which correspond to soft X-ray machines (Table 1). The first set describes an FEL driven by a laser-plasma accelerator ([3]) while the second set corresponds to a machine that utilizes the beam from the proposed PEP-X USR. For the LPA parameters, we start by considering a dispersion  $\eta = 3.5$  mm (for which  $\sigma_T/\sigma_x = 3.25$ ). Using the parallel beam model - Eq. (19) or (20) - we study the variation of the main properties of the fundamental mode with respect to the detuning parameter. In particular, in Fig. 1, we plot the negative imaginary part of the scaled, fundamental growth rate  $\mu_0 = \mu/(2\rho k_u)$  as a function of the scaled detuning  $\hat{\nu} = \Delta\nu/(2\rho)$  while

Table 1: Undulator and Electron Beam Parameters

Parameter	LPA	USR
Undulator parameter $K_0$	2	3.68
Undulator period $\lambda_u$	1 cm	2 cm
beam energy $\gamma_0 m c^2$	1 GeV	4.5 GeV
Resonant wavelength $\lambda_r$	3.9 nm	1 nm
Peak current $I_p$	10 kA	200 A
Energy spread $\sigma_\delta$	$10^{-2}$	$1.5 \times 10^{-3}$
Normalized emittance $\gamma_0 \epsilon_x$	$0.1 \mu\text{m}$	$0.0123 \mu\text{m}$
Normalized emittance $\gamma_0 \epsilon_y$	$0.1 \mu\text{m}$	$1.23 \mu\text{m}$
Horizontal size $\sigma_x$	$11.3 \mu\text{m}$	$8.3 \mu\text{m}$
Vertical size $\sigma_y$	$11.3 \mu\text{m}$	$38.7 \mu\text{m}$

Fig. 2 shows the frequency dependence of the scaled mode sizes. For  $\hat{\nu} \approx -0.5$ , the growth rate has a maximum value  $-\Im[\mu_0]_{max} \approx 0.28$ . This corresponds to a frequency-optimized gain length  $L_g = \sqrt{3}L_0/(2|\Im[\mu_0]|) \approx 22.3$  cm, where  $L_0 = \lambda_u/(4\pi\sqrt{3}\rho) \approx 7.3$  cm is the 1D gain length. Moreover, we note that the mode size in both  $x$  and  $y$  increases as we move towards longer wavelength (negative detuning). The analytical formula of Eq. (20) greatly facilitates the fast calculation of the frequency-optimized gain length as a function of the dispersion. The results are shown in Fig. 3, once more for the LPA parameters. For comparison, we have also included optimized gain length values derived from the 1-D formula ([3])

$$L_g \approx \frac{\lambda_u}{4\pi\sqrt{3}\rho_T} \left[ 1 + \frac{(\sigma_\delta^{ef})^2}{\rho_T^2} \right], \quad (22)$$

where we use the approximation  $\sigma_\delta^{ef} \approx \sigma_x/\eta$ . As expected, the gain length estimates from the 3-D theory are larger than their 1-D counterparts. However, the functional behavior is the same in both cases, in that the optimized

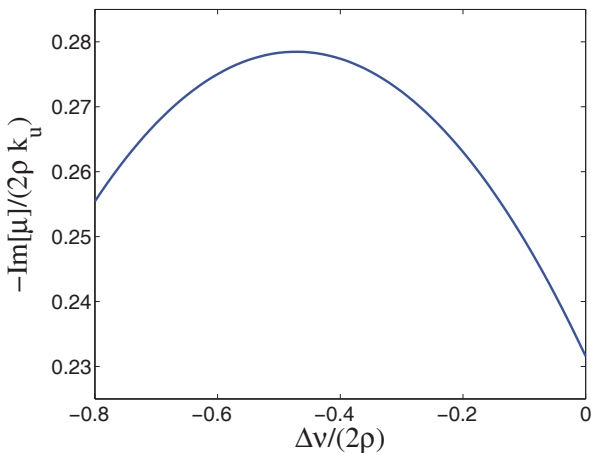


Figure 1: Negative imaginary part of the fundamental FEL growth rate  $\mu$  (in units of  $2\rho k_u$ ) as a function of the detuning  $\Delta\nu$  (in units of  $2\rho$ ) for  $\eta = 3.5$  mm (LPA set).

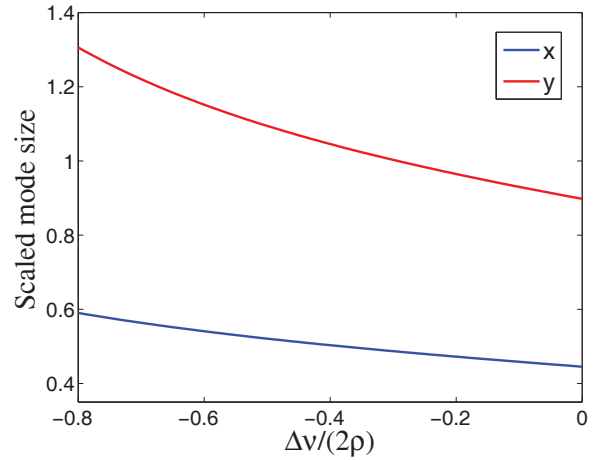


Figure 2: Scaled mode sizes as a function of detuning. In particular, the blue curve shows the variation of  $\sigma_{rx}/\sigma_T$  while the red one corresponds to  $\sigma_{ry}/\sigma_y$  ( $\eta = 3.5$  mm, LPA set).

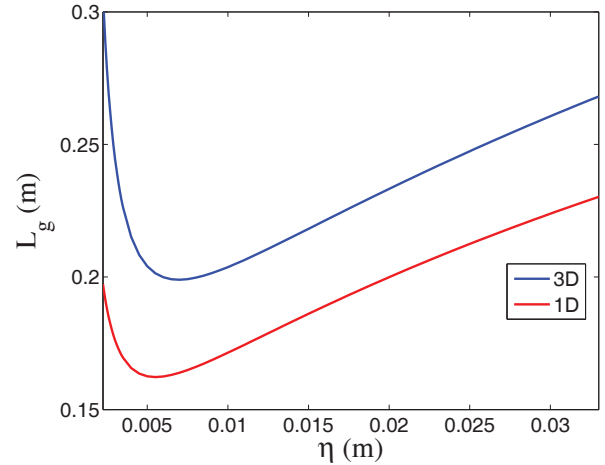


Figure 3: Frequency-optimized gain length as a function of dispersion for the LPA parameters. The data shown were derived using the parallel beam theory (blue) and the 1D formula - Eq. (22) - (red).

gain length attains a minimum for a particular dispersion (5-7 mm in our case). For dispersion values smaller than the optimal (where the effective energy spread is still large), the gain length curve is considerably steeper than for large  $\eta$ , where the large horizontal beam size eventually dominates the variation of  $L_g$ . Lastly, we note that for  $\eta = 1$  cm, we obtain an optimized gain length of slightly more than 20 cm. This agrees with the SASE simulations in [3], which showed saturation within 5 m of undulator for this dispersion value.

Next, we consider the parameters of the TGU FEL based on the PEP-X storage ring. In this case, we note that the undulator structure is rotated so that its  $x$  direction (in which we introduce the dispersion and the field gradient) becomes

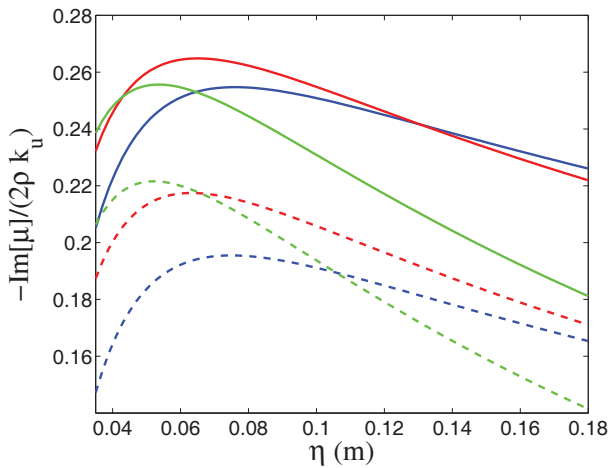


Figure 4: Scaled FEL growth rate as a function of dispersion for  $\Delta\nu/(2\rho) = 0.0/-0.2/-0.4$  (blue/red/green-USR set). Included are data from a parallel beam analysis (solid lines) and the model which includes vertical emittance and focusing (dashed lines).

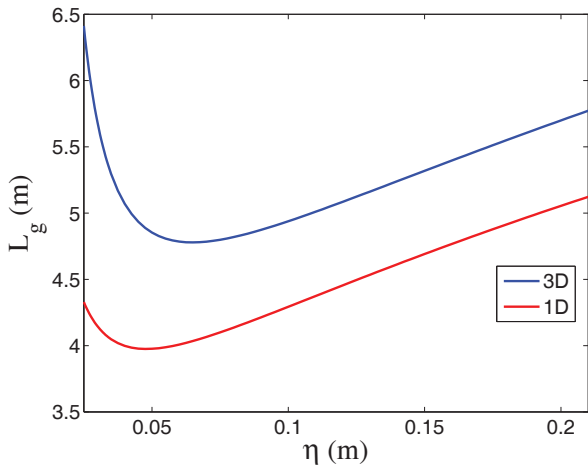


Figure 5: Frequency-optimized gain length as a function of dispersion for the USR example, using the parallel beam theory (blue) and the 1D formula (red).

perpendicular to the horizontal plane of the ring. This is done in order to take advantage of the much smaller equilibrium emittance in the vertical plane of the ring. In Fig. 4, we plot the scaled growth rate in terms of the dispersion for different values of the detuning, using both the parallel beam theory and the model which takes into account vertical emittance and undulator focusing. It becomes evident that the FEL growth rate is suppressed due to the added emittance effect. Overall, we obtain a maximum scaled growth rate  $-\Im[\mu_0]_{max} \approx 0.265$  from the parallel beam theory (which translates into a gain length  $L_g \approx 4.8$  m) while emittance reduces this value by about 20%. These observations agree with the results of a more rigorous optimization, given in Fig. 5.

### CONCLUSION

We have developed a theoretical framework for the study of a TGU-based, high gain FEL which takes into account three-dimensional effects such as emittance and undulator focusing. Whenever possible, we obtain a simplified description in terms of the FEL eigenmodes, which are determined through a variational technique. For small enough emittance, we use a parallel beam model which yields analytical expressions and facilitates the fast calculation of the mode properties. The results of our analysis are then used in optimization studies for two soft X-ray TGU FEL configurations.

### REFERENCES

- [1] T. Smith *et al.*, J. Appl. Phys. 50, 4580 (1979).
- [2] N. Kroll *et al.*, IEEE Journal of Quan. Electro. QE-17, 1496 (1981).
- [3] Z. Huang, Y. Ding and C. Schroeder, PRL 109, 204801 (2012)
- [4] P. Baxevanis, Y. Ding, R.D. Ruth and Z. Huang, to be published.
- [5] Z. Huang and K.-J. Kim, Phys. Rev. ST Accel. Beams 10, 034801 (2007).
- [6] P. Baxevanis, R. Ruth, Z. Huang, Phys. Rev. ST-AB 16, 010705 (2013).
- [7] M. Xie, Nucl. Instr. and Meth. A 507 (2003) 450.